Stability, reconstruction, and surface electronic states of group-III atoms on SiC(111)

Ulrike Grossner,* J. Furthmüller, and F. Bechstedt
Institut für Festkörpertheorie und Theoretische Optik, Friedrich-Schiller-Universität, Max-Wien-Platz 1, D-07743 Jena, Germany

(Received 30 January 2001; published 5 October 2001)

The adsorption of 1/3 monolayer of the group-III elements B, Al, Ga, and In on a Si-terminated SiC(111) $\sqrt{3}\times\sqrt{3}$R30° surface is investigated in dependence on the surface preparation conditions using the density functional theory (DFT). The energetics, the bonding behavior and the resulting surface electronic structure are studied and chemical trends are derived. For the metal atoms Al, Ga, and In the replacement of a Si atom in a T_4 position always gives the most stable configuration. The first-row element B shows a completely different behavior. Under Si-rich conditions boron replaces a second-layer C atom in a S_5 position, whereas under C-rich conditions a first-layer Si atom is replaced by boron. The different adsorbate configurations result in completely different surface electronic structures. Al, Ga, and In adsorption passivates the surface. The fundamental gap is virtually free from empty or occupied surface states. The B adsorption in the S_5 configuration follows this behavior. However, boron substituting a Si-atom gives rise to an empty midgap surface band.

DOI: 10.1103/PhysRevB.64.165308 PACS number(s): 68.35.Bs, 73.20.At, 68.35.Md

I. INTRODUCTION

Silicon carbide (SiC) is a wide-band-gap semiconductor with numerous technological applications in microelectronic devices that require high-temperature, high-frequency, or high-power operation. Interestingly more than 200 SiC polytypes exist with different stackings of the atomic Si-C bilayers in cubic [111] and hexagonal [0001] direction, respectively.[1] The variation of the fundamental energy gap by about 1 eV between the cubic zinc blende ($3C$) polytype and hexagonal (nH) polytypes with n Si-C bilayers in an unit cell[2] suggest the fabrication of heteropolytypic devices with active interfaces consisting of chemically identical but structurally different materials.[3,4] However, the homoepitaxial growth of different polytypes on each other is a hard challenge, although substantial progress has been demonstrated by means of solid-source molecular beam epitaxy (MBE).[5]

The change of the bilayer stacking and, hence, the polytype during epitaxial growth can be supported by a deliberate introduction of a surfactant that alters the free energy of the growing surface.[6] The realization of this idea has been demonstrated during homoepitaxy of silicon using boron, B, as a surfactant.[7,8] Locally the hexagonal wurtzite polytype $2H$ can be grown by a periodic arrangement of twin boundaries along the [111] direction. Indeed, during epitaxial growth of Si on a Si(111) $\sqrt{3}\times\sqrt{3}$R30°-B surface, a twin boundary is formed at the interface.[7,8] The question arises whether the other group-III elements Al, Ga, and In with the same valence-electron structure but different sizes and cores may also behave as surfactants.

$3C$-SiC(111) or nH-SiC(0001) surfaces chemisorbed by group-III elements Al, Ga, and In can be considered as prototype metal-semiconductor systems in analogy to the corresponding metal-silicon systems.[9] At a coverage of one third of a monolayer, chemisorption of the group-III elements on a surface like Si(111) leads to the formation of $\sqrt{3}\times\sqrt{3}$R30° structures.[9] Being trivalent, each group-III atom is expected to saturate three dangling bonds of the group-IV atoms on a (111) or (0001) surface.

In this article, we investigate the influence of the B, Al, Ga, and In adsorption on the surface structure and the electronic structure of a Si-terminated SiC(111) surface by means of *ab initio* calculations. Because of the three valence electrons of the group-III atoms the SiC(111) $\sqrt{3}\times\sqrt{3}$-III adsorbate is considered as prototypical surface. The stability of certain adatom configurations are investigated in dependence on adatom sizes and the surface preparation. The methods used are described in Sec. II. In Sec. III an extended discussion of the results is presented. Chemical trends are derived. Finally, a brief summary and conclusions are given in Sec. IV.

II. COMPUTATIONAL METHODS

The numerical studies are based on the density functional theory (DFT) within the local density approximation (LDA).[10] The electron-electron interaction is described within the Ceperley-Alder scheme as parametrized by Perdew and Zunger.[11] The interaction of the electrons with the atomic cores is treated by non-normconserving *ab initio* Vanderbilt pseudopotentials.[12] They allow a substantial potential softening for the first-row element C with the lack of core p electrons. As a consequence the plane-wave expansion of the single-particle eigenfunctions may be restricted by an energy cutoff of 13.4 Ry.[13] The eigenvalues and eigenfunctions of the single-particle Kohn-Sham equation[10] are taken to calculate the total energy of the system. Our calculations employ the conjugate-gradient method to minimize the total energy with respect to all degrees of freedom. Explicitly we use the Vienna *ab initio* simulation package.[15] For a bulk of the zinc blende polytype we obtain a cubic lattice constant of 4.332 Å and an indirect energy gap of 1.33 eV within DFT-LDA.

In order to study the group-III adsorbates we restrict the considerations to the prototypical cubic polytype $3C$ of SiC. We found the polytype influence on the structure and ener-

0163-1829/2001/64(16)/165308(7)/$20.00 ©2001 The American Physical Society

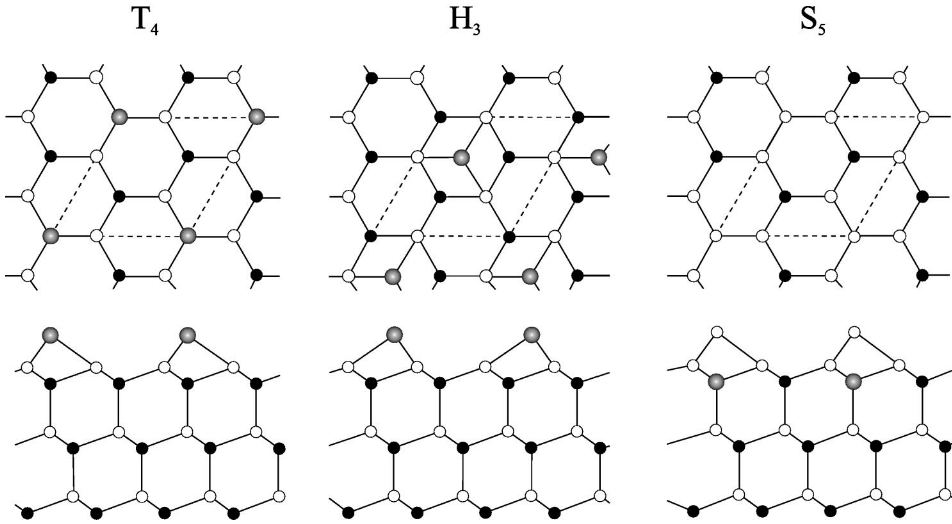

FIG. 1. Top view (upper panels) and side view (lower panels) of the standard adsorption structures T_4, H_3, and S_5 on a (111) surface. Here a Si-terminated SiC(111) surface is shown with Si atoms (open circles) and C atoms (dots). The shadowed circles indicate the group-III adatoms.

getics of the surface to be negligible.[13,14] The main difference is related to the position of the lowest unoccupied states due to the gap opening by about 1 eV in the case of the hexagonal polytypes. The adsorbate structures are restricted to surfaces with 1/3 monolayer of the considered group-III element. According to the experience with the Si(111) surfaces[9] and the trivalent character of the adsorbate atoms only overlayers with one third of a monolayer should lead to the formation of stable structures with $\sqrt{3}\times\sqrt{3}$R30° translational symmetry.

The Si-terminated $3C$-SiC(111) surfaces are modelled by repeated slabs containing six Si-C bilayers. A vacuum region of about the same thickness is taken into account. The C-terminated bottom layers of the resulting polar slabs are saturated by atomic hydrogen. The C-H bond length was found to be about 0.99 Å. During the total-energy optimization the coordinates in the lower C-terminated half of the slab are kept fixed in their ideal bulk positions, whereas the uppermost six surface bilayers are fully relaxed. The integrals over the surface Brillouin zone (BZ) are replaced by summation over six special points of the Monkhorst Pack type[16] in the irreducible part.

Since a compound semiconductor is studied, the group-III adsorption may depend on the surface preparation conditions. Despite of the fact that the adsorbate coverage is fixed to be one third of a monolayer and results in a $\sqrt{3}\times\sqrt{3}$R30° translational symmetry, the number N_X of $X=$Si,C atoms in the surface region may vary with the preparation. In the near thermal equilibrium the variation of the preparation conditions can be described by the actual chemical potentials μ_X of the surface constituents $X=$Si,C. The corresponding thermodynamical potential is the grandcanonical one.[17] In the low-temperature limit and with respect to the surface unit cell one has to study the surface energy

$$\Omega=E_{\rm tot}-\mu_{\rm Si}N_{\rm Si}-\mu_C N_C \tag{1}$$

with the total energy (TE) $E_{\rm tot}$ of the considered slab. For given preparation conditions $\mu_{\rm Si}$ and $\mu_{\rm C}$ the thermodynamically stable surface structure follows by minimization of the surface energy. Since the bulk solid SiC with the chemical potential $\mu_{\rm SiC(bulk)}$ is a reservoir which can exchange atoms with the surface, the mass action law, $\mu_{\rm Si}+\mu_{\rm C}=\mu_{\rm SiC(bulk)}$, holds. It allows the representation of the surface energy Ω Eq. (1) as a function of either $\mu_{\rm Si}$ or $\mu_{\rm C}$. The bulk energy per pair, $\mu_{\rm SiC(bulk)}=\mu_{\rm Si(bulk)}+\mu_{\rm C(bulk)}-\Delta H_f({\rm SiC})$, is equal to the sum of the energies of bulk elemental Si and C minus the heat of formation. The formation enthalpy is calculated to $\Delta H_f({\rm SiC})=0.58$ eV using the values $\mu_{\rm C(bulk)}$ and $\mu_{\rm SiC(bulk)}$ calculated for diamond and zinc blende SiC. The corresponding experimental value is $\Delta H_f({\rm SiC})=0.68$ eV.[18] The use of the cubic phases for the calculation of $\mu_{\rm C(bulk)}$ and $\mu_{\rm SiC(bulk)}$ is allowed since the differences between the cohesive energies of diamond and graphite are negligible.[13] The same holds for the various SiC polytypes.[19] The bulk chemical potential $\mu_{X({\rm bulk})}$ gives the upper limit of the chemical potential of a constituent $X={\rm Si,C},\mu_X\leqslant\mu_{X({\rm bulk})}$. Hence, with the mass-action law the thermodynamically allowed region of the potential fluctuation $\Delta\mu_X=\mu_X-\mu_{X({\rm bulk})}$ is defined by the interval $-\Delta H_f({\rm SiC})\leqslant\Delta\mu_X\leqslant 0$. Si-rich (C-poor) preparation conditions correspond to $\Delta\mu_{\rm Si}=0$, whereas $\Delta\mu_{\rm Si}=-\Delta H_f({\rm SiC})$ describes Si-poor (C-rich) conditions.

The TE calculations are performed for a variety of adsorbate structures. The threefold-coordinated standard adatom positions on a SiC(111) $\sqrt{3}\times\sqrt{3}$R30° surface are referred to as T_4 and H_3 sites (cf. Fig. 1, left and middle panel). They are known from the group-III metal adsorption on Si(111).[9] The T_4 site lies directly above a second-layer carbon atom, while the H_3 site is above a fourth-layer carbon atom. In the boron case, the most stable structure on the Si(111) $\sqrt{3}\times\sqrt{3}$R30° surface, on the other hand, has been found to be the so-called S_5 geometry (see Fig. 1, right panel) where the B atom substitutes for a second-layer carbon atom directly below the T_4 site, and the T_4 site is occupied by a silicon atom.[7,8,20] Moreover, adsorbate structures with an additional Si atom are studied. They are characterized by two adatom sites. For instance, a T_4(Si)+H_3(B) system corresponds to a surface structure with one Si adatom at a T_4 site, whereas the boron atom occupies a H_3 site.

Because of the covalent radius of boron one expects a preferential replacement of a carbon atom, i.e., an adsorption

at a S_5 site. Nevertheless, we also consider a situation where a B adatom replaces a Si atom belonging to the three basis atoms of the Si adatom in a T_4 position. We call such an adsorbate geometry as sub-S_4 site. Since, in addition the Si adatom in a T_4 position also a Si adatom at a H_3 site can be considered, we differ between T_4(Si)+sub-S_4(B) and H_3(Si)+sub-S_4(B) overlayer geometries. In addition, we also consider adsorbate configuration $S_5(\mathrm{H}_3)$ and sub-$S_4(\mathrm{H}_3)$, where the Si adatom occupies a H_3 site instead of a T_4 position.

III. RESULTS AND DISCUSSION

A. Energetics

The surface energies Ω of the considered 11 adsorbate configurations are presented in Fig. 2 versus the variation $\Delta\mu_{\mathrm{Si}}$ of the Si chemical potential with respect to its bulk value. In the boron case the standard adatom configurations H_3 and T_4 as well as their combinations with an additional Si adatom are energetically unfavorable. Rather, the incorporation of a B atom in the subsurface region connected with an exchange of a C atom in the second atomic layer below the T_4 site (i.e., S_5) or a Si atom in the first atomic layer bonded to the T_4-Si adatom (i.e., sub-S_4) gives the lowest-energy configurations. The occurrence of a substitutional S_5 adsorption site in Fig. 2, upper panel, under Si-rich preparation conditions is in complete agreement with the theoretical and experimental findings for the Si(111)$\sqrt{3}\times\sqrt{3}$R30° surface.[20–26] Under less Si-rich surface preparation conditions the situation changes dramatically. Here, boron substitutes a Si basis atom of the Si adatom in a sub-S_4 position. Until now there are no experimental observations of this fact. However, it seems that boron impurities exhibit a similar behavior in a bulk environment.[27]

In the case of adsorption of the metal atoms Al, Ga, and In the occupation of the T_4 site is the most favorable one (see Fig. 2, lower panels). Adsorption in a H_3 site above a fourth-layer carbon atom gives rise to a higher surface energy by 0.7 (Al), 0.6 (Ga), and 0.4 eV (In). The surface energy of the adsorption of an additional Si atom in a H_3 position (H_3+T_4 structure) comes close to that of the most favorable T_4 configuration for very Si-rich preparation conditions, at least for Ga and In. In the Al case this configuration relaxes to a kind of a bridge site and a top site for the Al atom, as indicated by Bridge(Si) $+T_1$(A l). The aluminum atom forms a direct bond with the underlying Si atom. Such an adatom configuration has been already discussed for the Si(111) surface.[28] The energy gain may be a consequence of the strong Al-Si bond, even if the long-range adsorbate interaction gives rise to an opposite tendency.

The explanation of the different adsorption behaviors follows the chemical bonding as already discussed for Si(111) surfaces.[20] The favorization of a T_4 site versus a H_3 site is a consequence of the shorter group-III-Si bonds, in particular in the (111) plane. In the T_4 geometry the metal adatom transfers charge to its three nearest-neighboring silicon atoms. This results in an attractive Coulomb interaction between adatom and the uppermost Si atomic layer. In the S_5

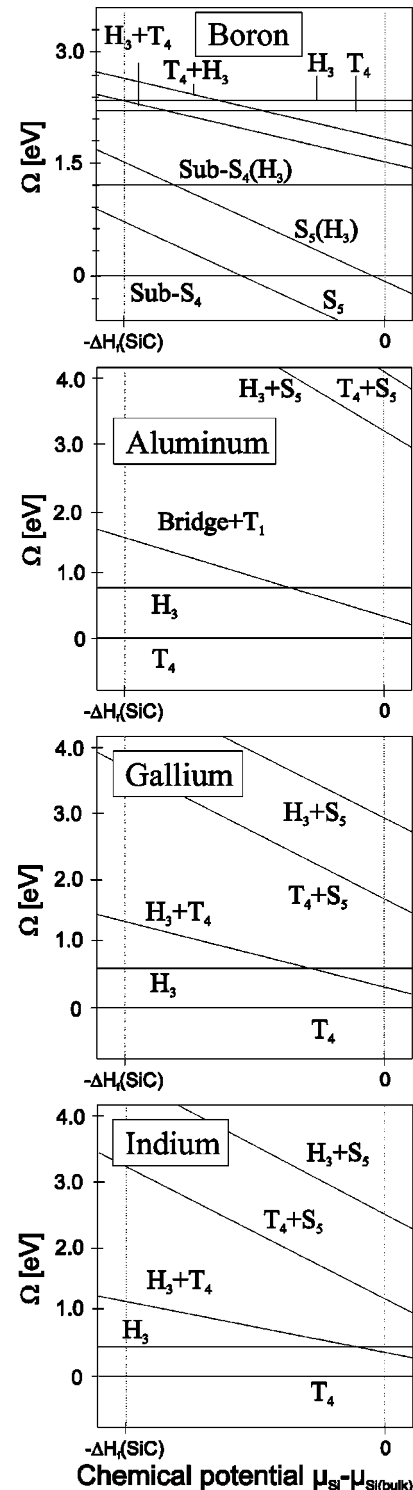

FIG. 2. Surface energy versus the variation of the Si chemical potential for various adsorbate configurations of boron, aluminum, gallium, and indium. The thermodynamically allowed range is indicated by dashed lines. The sub-S_4 (T_4) adsorption configuration of boron (aluminum, gallium, indium) is used as energy zero.

configuration, both the Si adatom and the metal atom on a C site transfer electrons to the neighbors. As a consequence a Coulomb repulsion between Si adatom and metal atom occurs, making this configuration unfavorable. In the case of

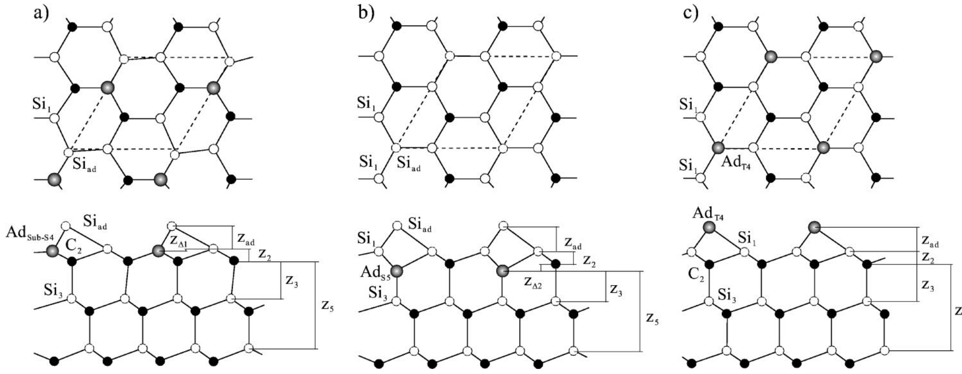

FIG. 3. (a) Top and side view of a sub-S_4 adsorption site on a SiC(111)$\sqrt{3}\times\sqrt{3}$R30° surface. (b) Top and side view of a S_5 adsorption site. (c) Top and side view of a T_4 adsorption site. Open circles: Si atoms, filled circles: C atoms, shadowed circles: group-III atom. Important atomic sites and atomic distances parallel to the (111) direction are indicated.

the boron coverage the charge transfers are substantially reduced, allowing a reversed energetical ordering.

B. Geometry

The most important geometry parameters of the energetically favorable adsorbate structures sub-S_4, S_5, and T_4 are indicated in Figs. 3(a)–3(c). The values of the geometry parameters are listed in Tables I and II. They are the bond length $d(\mathrm{Si}_{ad})$ $[d(\mathrm{III}_{ad})]$ between Si or group-III adatom in T_4 position and a neighboring Si atom, $d(\mathrm{Si}_1)$ between B in S_5 position and a first-layer Si atom, $d(\mathrm{C}_2)$ between B or Si in sub-S_4 position and a second-layer carbon atom, $d(\mathrm{Si}_3)$ between B or C in S_5 and a third-layer Si atom. The parameters z_{ad}, $z_{\Delta 1}$, z_2, $z_{\Delta 2}$, z_3, and z_5 describe vertical layer separations between two atomic layers parallel to the (111) direction. We have to mention that all these values suffer from the slight LDA overbinding effect as indicated by the computed lattice constant $a_0=4.332$ Å of the cubic SiC in comparison to the experimental one $a_0=4.360$ Å.[19]

In the case of the sub-S_4 (S_5) boron adsorbate structures the values $d(\mathrm{Si}_{ad})=2.24$ (2.16) Å and $z_{ad}=1.38$ (1.55) Å come close to the values of the pure SiC(111)$\sqrt{3}\times\sqrt{3}$R30° overlayer with values 2.43 and 1.74 Å.[14] Only the adclusters are somewhat compressed. The bond length $d(C_2)=1.65$ Å between the B atom and a carbon atom in the second atomic layer only slightly overestimates the value for a single C-C bond. The B-Si bond lengths $d(Si_1)=1.90$ Å and $d(Si_3)=1.90$ Å in the S_5 structure are dominated by the characteristic bond length in the bulk SiC. The interlayer distances z_2, z_3, and z_5 in Table I approach the values found for the pure SiC surface.[14] However, the boron adsorption induces the layer bucklings $z_{\Delta 1}$ or $z_{\Delta 2}$. Interestingly the geometry parameters in the uppermost layers of the S_5 structure are not very different from those for the B adsorption on Si(111)$\sqrt{3}\times\sqrt{3}$. Photoelectron diffraction[26] gave the values $d(\mathrm{Si}_{ad})=2.21$ Å and $d(\mathrm{Si}_3)=1.98$ Å.

In the case of the stable T_4 adsorbate structures (see Table II) the characteristic bond lengths $d(\mathrm{III}_{ad})$ and $d(C_2)$ clearly follow the increase with the covalent radius of the group-III metal. The sum of the covalent radii $r_{Si}+r_{\mathrm{III}}$ amounts to 2.19 Å (Al), 2.37 Å (Ga), and 2.55 Å (In).[29] A similar increase is observable for the vertical distance z_{ad} of the adatom from the SiC(111) surface. The layer spacings z_2, z_3, and z_3 are rather independent of the adsorbate species. Their values are close to the findings for a clean SiC(111)$\sqrt{3}\times\sqrt{3}$ surface with $z_2=0.63$ Å, $z_3=1.89$ Å, and $z_5=4.38$ Å.[14]

TABLE I. Structural parameters of the energetically most favorable B adsorbate configurations. All values are given in units of Å.

Parameter	sub-S_4	S_5
d (Si_{ad})	2.24	2.16
d (Si_1)		1.90
d (C_2)	1.65	
d (Si_3)		1.90
z_{ad}	1.38	1.55
$z_{\Delta 1}$	0.27	
z_2	0.53	0.53
$z_{\Delta 2}$		0.04
z_3	1.91	1.90
z_5	4.43	4.36

C. Electronic structure

The adsorption of the group-III elements also influences the surface electronic structure. This is directly demonstrated in Fig. 4 which represents the charge density and the arrangement of aluminum, gallium, and indium atoms in a T_4 adatom position. The trivalent adatoms form bonds with the underlying Si basis atoms with strong covalent character. The partial ionic character of these bonds is indicated by the center of mass of the electron density that is slightly displaced towards the Si atoms. This is most clearly visible for the Al adsorption. In the case of Ga and In adsorption the plotted shallow Ga3d and In4d electrons reduce this impres-

TABLE II. Structural parameters of the most stable T_4 configuration of the group-III adsorption. All values are given in units of Å.

Parameter	Al	Ga	In
d (III_{ad})	2.44	2.46	2.65
d (C_2)	2.28	2.43	2.64
z_{ad}	1.68	1.73	1.98
z_2	0.60	0.59	0.59
z_3	1.90	1.90	1.89
z_4	4.41	4.41	4.41

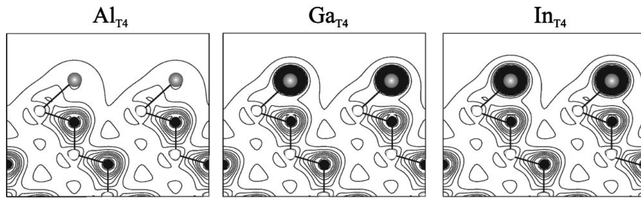

FIG. 4. Charge density projected onto a (110) plane of the Al-, Ga-, and In-covered SiC(111) $\sqrt{3}\times\sqrt{3}$R30° surface. Si atoms: open circles, C atoms: dots, group-III atoms: shadowed circles. Results are presented for the most stable adsorption geometry (T_4). Note that for Ga (In) the *3d-* (*4d-*) electrons are included as valence electrons.

sion. Again this bonding behavior is very similar to that found for Al, Ga, and In on the Si(111) $\sqrt{3}\times\sqrt{3}$ surface.[20,30]

The two different stable boron adsorbates give rise to completely different surface electronic structures. This is indicated by the surface band structures (cf. Fig. 5, first and second panel). For boron substituing a Si atom in the first-atomic layer under C-rich preparation conditions, i.e., the sub-S_4 configuration, an unoccupied band occurs in the middle of the fundamental gap. In DFT-LDA, i.e., without taking into account the excitation aspect, it is situated 0.3–0.7 eV above the valence band maximum (VBM). It is originated by an overlap of the empty dangling bonds situated at the Si adatom and the B-Si antibonding states of the back bond due to the nearest-neighbor interaction. In the case of the hexagonal polytypes we expect a similar behavior of the surface bands. Only the projected conduction bands should be shifted to higher energies by about 1 eV.

The surface-induced bands change completely for boron substituting a C atom under Si-rich conditions. For this S_5 adsorbate structure the fundamental gap almost remains empty. Close to the BZ boundary along the MK line occupied surface bands appear below the VBM. Unoccupied surface bands are observed near the CBM. They are to the Si dangling bonds and B-Si antibonding states. The situation is similar to the B adsorption on the Si(111) $\sqrt{3}\times\sqrt{3}$R30° surface.[30] The smaller distances of the empty surface band to the VBM is a consequence of the larger Si-B bond lengths.

The band structures of the group-III adatoms in a T_4 position (Fig. 5, lower panels) are rather similar to that of boron in a S_5 structure. With an energy of about that of the bulk VBM occupied surface bands occur along the MK line in the surface BZ as well as unoccupied surface bands around the CBM. In addition, there is a pronounced occupied surface band above the VBM at the high-symmetry point *M*. It shows significant chemical trends concerning energetical position and dispersion. The energetical position changes from a position above the VBM (Al) to a position below the VBM (Ga, In) and its dispersion decreases along the row Al, Ga, In of the adatom. This is mainly a consequence of the trend with the III-Si bond length and the overlap of group-III with bulk states.

An interesting quantity in all these band structures is the uppermost occupied state. Its distance to the vacuum level gives the ionization energy of the system. We extract this quantity using the local electrostatic potential that is aver-

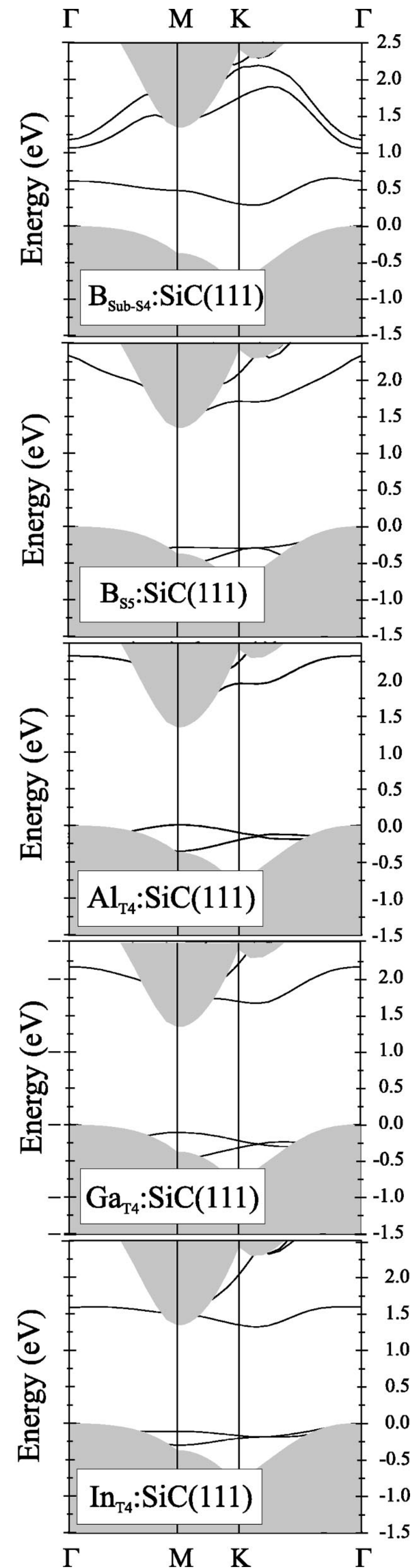

FIG. 5. Band structure of $\frac{1}{3}$ monolayer boron (aluminum, gallium, indium) adsorbates on the SiC(111) $\sqrt{3}\times\sqrt{3}$R30° surface. Results for the most stable adsorbate geometries are plotted. The projected band structure of the bulk cubic SiC is indicated by the shaded regions. Surface bands are indicated by solid lines versus the high-symmetry directions in the surface BZ.

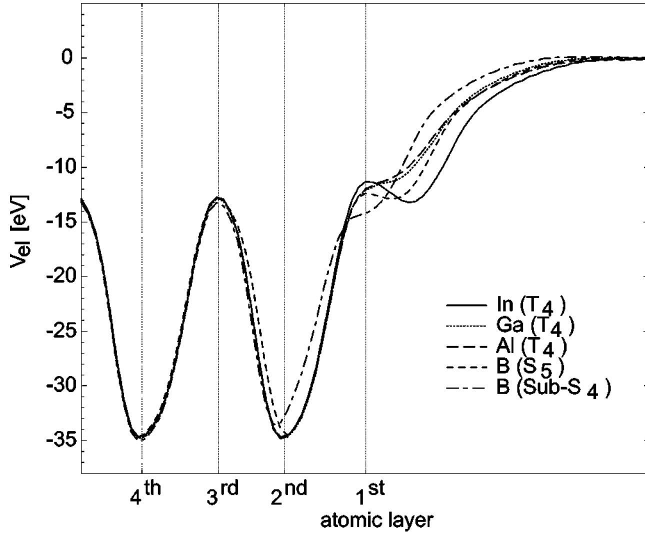

FIG. 6. Averaged electrostatic potential of differently covered SiC(111) $\sqrt{3}\times\sqrt{3}$R30° surfaces vs the bulk depth (arbitary units).

aged over the plane perpendicular to the (111) surface normal (see Fig. 6). The energetical distance between its vacuum position and the spatially averaged value in the bulk is defined by the dipole potential related to the displacements of the charges in the surface and, hence, strongly depends on the adsorbate geometry and the coverage. The surface dipole influences the ionization energy. It is obtained in DFT-LDA quality as the energetical distance of the highest occupied state and the asymptotic value of the electrostatic potential in the vacuum. In order to take into account also the excitation aspect the quasiparticle shift of the VBM towards lower energies has to be added. It amounts to about 0.64 eV (Ref. 31) for bulk cubic SiC.

Table III shows the ionization energies for the different adsorbate atoms and the corresponding adsorption sites. The geometries considered for the boron adsorption can be classified into three groups: two with B on top of the surface [T_4(Si)+H_3(B), H_3(Si)+T_4(B)], two with boron in the first surface layer [T_4(Si)+sub-S_4(B), H_3(Si)+sub-S_4(B)], and two with boron in the second surface layer [T_4(Si)+S_5(B), H_3(Si)+S_5(B)]. Owing to the accompanying charge transfer the ionization energies also decrease from values close to the surface with a Si atom at the T_4 site (4.35, 4.38 eV) over 4.13 eV [i.e., T_4(Si)+sub-S_4(B)] to about 3.91 eV [T_4(Si)+S_5(B)]. The ionization energies of the geometries considered for the Al adsorption on SiC(111) $\sqrt{3}\times\sqrt{3}$R30° vary only little with the different adsorption sites. The main reason is that aluminum always occurs on top of the surface. The corresponding ionization energy of 4.4 eV of the clean SiC(111) $\sqrt{3}\times\sqrt{3}$R30° is by about 0.4–0.5 eV larger, since here an additional electron is localized at the Si adatom. For Ga and In a similar behavior is found. Hence, only the values for the most stable adsorption site T_4 are listed. A comparison of the ionization energies of the three similar adsorption sites of Al, Ga, and In shows the largest surface dipole for the Ga adsorbate. This can be explained with the high electronegativity of Ga (1.8) compared to Al (1.5) and In (1.5).[32]

TABLE III. Ionization energies for different adsorbates and adsorbate geometries.

Adsorbate structure	Ionization energy (eV)
T4(Si)+H3(B)	4.35
H_3(Si)+T_4(B)	4.38
T_4(Si)+sub-S_4(B)	4.13
H_3(Si)+sub-S_4(B)	4.12
T_4(Si)+S_5(B)	3.91
H_3(Si)+S_5(B)	3.84
T_4(Al)	3.91
H_3(Al)	3.83
Bridge (Si)+T(Al)	3.96
T_4(Ga)	4.03
T_4(In)	3.64

IV. CONCLUSIONS

In conclusion, we have studied structural, thermodynamic and electronic properties of group-III adsorbates on a Si-terminated SiC(111) $\sqrt{3}\times\sqrt{3}$R30° surface. In these studies we have combined *first-principles* total energy optimizations and electronic-structure calculations with thermodynamical considerations. Explicitly a pseudopotential-plane-wave code has been used. As already found for the group-III-Si(111) systems the adsorption of boron or the group-III metals leads to completely different results because of the smaller covalent radius and the higher electronegativity of the B atoms compared to the corresponding properties of the metal atoms Al, Ga, and In.[29]

In the case of the boron adsorption we have observed two different stable adsorbate geometries depending on the surface growth conditions. Under Si-rich conditions the carbon-substituting S_5 site is energetically favorable, whereas under C-rich conditions a silicon-substituting sub-S_4 site is found. The results are in seemingly agreement with the behavior during B doping of bulk SiC crystals. For Al, Ga, and In we have found the adsorption on a T_4 adatom site to be favored. Al, Ga, and In give rise to a complete passivation of the SiC surface. The fundamental gap is virtually free of surface states.

This work has been supported by the Deutsche Forschungsgemeinschaft (Sonderforschungsbereich 196, project A8). Most of the computations have been done using the facilities of the J. v. Neumann Institute for Computing (NIC) at the Forschungszentrum Jülich.

*Present address: Institut für Festkörperphysik, Friedrich-Schiller-Universität, Max-Wien-Platz 1, 07743 Jena, Germany. Email address: ulrike@ifto.physik.uni-jena.de

[1] N. W. Jepps and T. F. Page, Prog. Cryst. Growth Charact. **7**, 259 (1983).
[2] W. J. Choyke, D. R. Hamilton, and L. Pattrick, Phys. Rev. **133**, A1163 (1964).
[3] M. Ruf, H. Hitlehner, and R. Helbig, IEEE Electron Device Lett. **41**, 1040 (1994).
[4] F. Bechstedt and P. Käckell, Phys. Rev. Lett. **75**, 264 (1995).
[5] A. Fissel, B. Schröter, and W. Richter, Adv. Solid State Phys. **38**, 87 (1999).
[6] M. Copel, M. C. Reuter, E. Kaxiras, and R. M. Tromp, Phys. Rev. Lett. **63**, 632 (1989).
[7] R. L. Headrick, B. E. Weir, J. Bevk, B. S. Freer, D. J. Eaglesham, and L. C. Feldman, Phys. Rev. Lett. **65**, 1128 (1990).
[8] H. Hibino, K. Sumitomo, and T. Ogino, J. Vac. Sci. Technol. A **16**, 1934 (1998).
[9] W. Mönch, *Semiconductor Surfaces and Interfaces* (Springer-Verlag, Berlin, 1993).
[10] P. Hohenberg and W. Kohn, Phys. Rev. **136**, B864 (1964); W. Kohn and L. J. Sham, Phys. Rev. **140**, A1133 (1965).
[11] J. P. Perdew and A. Zunger, Phys. Rev. B **23**, 5048 (1980).
[12] D. Vanderbilt, Phys. Rev. B **41**, 7892 (1990).
[13] J. Furthmüller, P. Käckell, F. Bechstedt, and G. Kresse, Phys. Rev. B **61**, 4576 (2000).
[14] F. Bechstedt, P. Käckell, A. Zywietz, K. Karch, B. Adolph, K. Tenelsen, and J. Furthmüller, Phys. Status Solidi B **202**, 35 (1997).
[15] G. Kresse and J. Furthmüller, Comput. Mater. Sci. **6**, 15 (1996); Phys. Rev. B **54**, 11 169 (1996).
[16] H. J. Monkhorst and J. D. Pack, Phys. Rev. B **13**, 5188 (1976).
[17] G.-X. Qian, R. M. Martin, and D. J. Chadi, Phys. Rev. Lett. **60**, 162 (1988); Phys. Rev. B **38**, 7649 (1988).
[18] W. A. Harrison, *Electronic Structure and the Properties of Solids* (Dover, New York, 1989).
[19] P. Käckell, B. Wenzien, and F. Bechstedt, Phys. Rev. B **50**, 17 037 (1994).
[20] S. Wang, M. W. Radny, and P. V. Smith, Phys. Rev. B **59**, 1594 (1999).
[21] I.-W. Lyo, E. Kaxiras, and Ph. Avouris, Phys. Rev. Lett. **63**, 1261 (1989).
[22] S. Wang, M. W. Radny, and P. V. Smith, Surf. Sci. **394**, 235 (1997).
[23] R. L. Headrick, I. K. Robinson, E. Vlieg, and L. C. Feldman, Phys. Rev. Lett. **63**, 1253 (1989).
[24] H. Huang, S. Y. Tong, J. Quinn, and F. Jona, Phys. Rev. B **41**, 3276 (1990).
[25] A. V. Zotov, M. A. Kulakov, S. V. Ryzhkov, A. A. Saranin, V. G. Lifshits, B. Bullemer, and I. Eisele, Surf. Sci. **345**, 313 (1996).
[26] P. Baumgärtel, J. J. Paggel, M. Hasselbarth, K. Horn, V. Fernandez, O. Schaff, J. H. Weaver, A. M. Bradshaw, D. P. Woodruff, E. Rotenberg, and J. Denlinger, Phys. Rev. B **59**, 13 014 (1999).
[27] T. Frank, T. Troffer, G. Pensl, N. Nordell, S. Karlsson, and A. Schöner, Mater. Sci. Forum **264-268**, 681 (1998).
[28] F. Illas, J. M. Ricart, J. Rubio, and J. Casanovas, Phys. Rev. B **47**, 2417 (1993).
[29] Sargent-Welch, *Table of Periodic Properties of the Elements* (Sargent-Welch Scientific Company, Skokie, Il, 1980).
[30] H. Nagayoshi, Surf. Rev. Lett. **1**, 369 (1994).
[31] B. Wenzien, P. Käckell, F. Bechstedt, and G. Cappellini, Phys. Rev. B **52**, 10 897 (1995).
[32] Periodensystem der Elemente, VCH Verlagsgesellschaft, Weinheim, 10 10 100 (1989).